Electrochimica Acta 150 (2014) 129–135

Contents lists available at ScienceDirect

Electrochimica Acta

journal homepage: www.elsevier.com/locate/electacta

Poly vinyl acetate used as a binder for the fabrication of a $LiFePO_4$-based composite cathode for lithium-ion batteries

Pier Paolo Prosini [a,b,*], Maria Carewska [a], Cinzia Cento [a], Amedeo Masci [a]

[a] ENEA, Italian National Agency for New Technologies, Energy and Sustainable Economic Development, Casaccia Research Centre, Via Anguillarese 301, 00123 Santa Maria di Galeria, Rome, Italy
[b] DInESto, Drive the Innovation in Energy Storage, Via Provincie, 04012 Cisterna di Latina, Italy

ARTICLE INFO

Article history:
Received 26 August 2014
Received in revised form 30 September 2014
Accepted 24 October 2014
Available online 28 October 2014

Keywords:
poly vinyl acetate
composite cathode
lithium battery
lithium iron phosphate

ABSTRACT

This paper describes a method for the preparation of composite cathodes for lithium ion-batteries by using poly vinyl acetate (PVAc) as a binder. PVAc is a non-fluorinated water dispersible polymer commonly used in a large number of industrial applications. The main advantages for using of this polymer are related to its low cost and negligible toxicity. Furthermore, since the PVAc is water processable, its use allows to replace the organic solvent, employed to dissolve the fluorinated polymer normally used as a binder in lithium battery technology, with water. In such a way it is possible to decrease the hazardousness of the preparation process as well as the production costs of the electrodes. In the paper the preparation, characterization and electrochemical performance of a $LiFePO_4$ electrode based on PVAc as the binder is described. Furthermore, to assess the effect of the PVAc binder on the electrode properties, its performance is compared to that of a conventional electrode employing PVdF-HFP as a binder.

1. INTRODUCTION

The electrodes used in lithium-ion battery technology are formed by an electro-active material, carbon and a polymer binder which primarily ensures the mechanical stability of the electrodes. The characteristics of the binding material are of vital importance for a correct functioning of the battery. The traditional polymer for producing electrodes for Li-ion batteries is the poly(vinylidene fluoride-co-exafluoropropylene) (PVdF-HFP). The production process (solvent-based) for the electrode manufacturing involves the following steps: mixing the powder of the active material with carbon, dissolving the PVdF-HFP with the solvent, mixing the powders with the solution to form a slurry, spreading the slurry on a current collector and drying the electrode while recovering the solvents [1]. N-methyl pyrrolidone (NMP) is the solvent commonly used to dissolve the PVdF-HFP. The aforementioned process for the preparation of electrodes has drawbacks, primarily due to the hazard connected with the use of NMP. NMP is a heterocyclic compound, which is liquid at room temperature. NMP boils at about 200 °C and its flammability limits are between 1.3 and 9.5% vol. NMP is part of the so-called volatile organic compounds (VOC). NMP is classified by the European Union as toxic. It is also classified in Categories 2 in terms of reproductive toxicity and it is irritant to eyes, respiratory system, and skin [2]. For these reasons NMP cannot be left free in the environment and must be recovered during the drying phase.

In recent years increasing environmental awareness and safety consciousness, as well as the intensification of the legislator's attention, has given rise to increasingly restrictive regulations aimed at limiting the use of VOCs in manufacturing processes. One of the possible alternatives to reduce the use of VOCs is the adoption of aqueous solutions or suspensions. For environmental consistency and cost considerations, the aqueous process is gaining favor and has attracted significant interest in the field of lithium batteries [3,4]. To make the aqueous route an appropriate alternative to the organic one, the chemical stability of the active material in water and the physical stability of the so obtained electrode have to be verified. The stability of $LiFePO_4$ in water was investigated by Porcher et al. [5]. From physical and chemical analyses, they showed that a thin Li_3PO_4 layer is formed at the $LiFePO_4$ grain surface after immersion in water. Nevertheless, no effect was observed on the electrochemical performance [6]. The aqueous processing of $LiFePO_4$-based electrodes being proved, the researchers concentrated their attention on the use of different polymers and surfactants. Several different polymers, individually or in mixture between them have been used as a binder. Porcher used polyvinyl alcohol and polyethylene glycol or a

* Corresponding author. Tel.: +39 06 3048 6768; fax: +39 06 3048 6357.
E-mail address: pierpaolo.prosini@enea.it (P.P. Prosini).

http://dx.doi.org/10.1016/j.electacta.2014.10.123
0013-4686/

butadiene–acrylonitrile copolymer rubber latex as the binder and hydroxyl propyl methyl cellulose and carboxyl methyl cellulose as the thickener [7]. Guerfi et al. [8] reported on the characterization of $LiFePO_4$ cathode using a new water-soluble binder obtained from ZEON Corp., based on saturated organic compounds. Lee et al. used carboxymethyl cellulose and poly(acrylic acid) as a binder [9]. The effects of dispersants such as poly(4-styrene sulfonic acid), poly (ammonium acrylate), and poly(acrylic acid-co-maleic acid) on the dispersion and electrochemical properties of carbon-coated lithium iron phosphate cathodes were studied by Li et al. [10,11]. Carboxymethyl chitosan was recently reported as a water soluble binder for $LiFePO_4$ cathode in Li-ion batteries by Sun et al. [12]. In order to reduce both the electrode and the process costs we tried to use PVAc as a binder for the fabrication of cathodes for lithium-ion batteries. PVAc is a not toxic thermoplastic resin produced by the polymerization of vinyl acetate monomer [$CH_3COOCHCH_2$] in water producing an emulsion with a solids content of 50–55%. PVAc is a polymer with unique physical and chemical properties. Since its discovery in 1915 by Klatte [13], it has found many applications and new areas of interest are still being added. The aim of the present work is to study a process for making positive electrodes for lithium-ion batteries using PVAc as a binder. PVAc was chosen because it is stable, non-flammable and not hazardous health-wise product (hazard category 0 according to the National Fire Protection Association standards for all danger categories). It is water dispersible and, furthermore, its cost is very competitive when compared to other polymers.

2. EXPERIMENTAL

2.1. Preparation of the PVAc-based cathode

The preparation described herein refers to a 100 cm^2 of cathode tape. Lithium iron phosphate (Gelon lib Group, ShanDong, P.R. China) and carbon black (Super P, MMM, Belgium) were used as the active material and the conductive agent, respectively. 1.5 g of lithium iron phosphate and 0.25 g of carbon black were weighed and transferred to a mechanic mill (Mixer Mill MM200, Retsch) and mixed by operating the device for a few minutes. PVAc with a solid mass fraction of 50% was used (Vinavil SpA via Valtellina, 63 - 20159 Milano - Italia). 0.5 g of PVAc was dispersed in 5 g of water. The dispersion of PVAc was subsequently added to the powder mixture and the components were mixed by operating the mill for a few minutes. The so obtained suspension was used to paint a thin aluminum sheet covering a surface area of 100 cm^2. After drying in air at 130–150 °C, the procedure was repeated as many times as was necessary to use up the entire suspension. A typical PVAc-based cathode tape composition was 75 wt.% $LiFePO_4$, 12.5 wt.% PVAc, and 12.5 wt.% SuperP.

2.2. Preparation of PVdF-based cathode

Poly (vinylidene difloruro-co-hexa fluoropropylene) copolymer (PVDF-HFP, Aldrich) was used as a binder and dibutyl phthalate (BDH) as a plasticizer. The amount of plasticizer was 5% of the electrode mass. The ratio between the active material and the electronic conductor was set to 8:1. The amount of PVDF-HFP was 10 wt.%. For the electrode preparation, the active material and the carbon were weighted in the right proportions and extensively mixed by using the Mixer Mill MM200. A binder solution was prepared by dissolving 5 wt.% of PVDF-HFP in cyclohexanone to obtain a homogeneous solution. To facilitate the dissolution of the polymer, the solution was heated at 70 °C. The active material/carbon mixture was added to the binder solution contained in a Teflon jar of a capacity of about 50 cm^3, equipped with two Teflon spheres of 13 g in weight. The total amount of slurry in the jar was about 18–20 g. The jar was placed in a planetary mill (Retsch). The jar was mixed for 4 hours at 60% of the maximum power of the mill followed by 12 hours of milling at 15% of the maximum power. The slurry was spread by means of a calibrated slots (RK Print-Coat Instruments Ltd.) on an aluminum support and dried in air. To remove the plasticizer the cathode tape was heated at 110 °C for 16 h. The PVdF-based cathode tape composition was 80 wt.% $LiFePO_4$, 10 wt.% PVdF-HFP, and 10 wt.% SuperP.

2.3. Chemical-physical characterization

The morphology and composition of the PVAc tape were evaluated by scanning electron microscopy (SEM). High magnification microphotographs were obtained by means a Jeol JSM-5510LV. The surface chemistry was mapped with an X-ray energy dispersive spectroscopy (EDS) system (IXRF EDS-2000). The specimens were directly mounted onto a conductive carbon double face tape, which was previously assembled on a slab. The density of the materials was determined by using a helium pycnometer (Accupyc Micromeritics).

2.4. Thermal characterization

Thermal stabilities of the PVAc-based tape were verified under nitrogen using a simultaneous TG-DTA (Q600 SDT, TA Instruments) equipped with the Thermal Solution Software (version 1.4). The temperature was calibrated using the nickel Curie point as the reference. The mass was calibrated using ceramic standards provided with the instrument. High purity aluminium oxide was used as the reference material. Open platinum crucibles (cross-section = 0.32 cm^2) were used to contain the samples. The experiments were performed on 10–12 mg samples that were stored, handled, and weighed in a dry-room. The thermal stability was investigated by heating the samples from room temperature up to 750 °C at a rate of 10 °C min^{-1}. The onset temperature was calculated by thermal analysis software (Universal Analysis version 2.5) as the intersection between the extrapolated baseline weight and the tangent through the inflection point of the weight vs. temperature curve.

2.5. Electrochemical Characterization

For the electrochemical characterization, electrodes were punched from the cathode tapes in the form of discs. The PVAc-based electrodes had a diameter of 10 mm and a weight of 10.2–17.6 mg. The weight of the active material into the electrode ranged between 7.6 and 13.2 mg. The PVdF-based electrode had a diameter of 10 mm and a weight of 13.0 mg. The weight of the active material into the electrode was 10.4 mg. The cycling performance and life of cells containing the electrodes were examined in 2032-type coin cells. Prior of the electrochemical characterization the electrodes were dried by heating under vacuum at 110 °C. To evaluate the electrode properties, two electrodes lithium cells were prepared in which lithium acted as the counter and reference electrode. A glass fiber was used as the separator. Coin cells were filled with a 1.0 M solution of $LiPF_6$ in ethylene carbonate/diethyl carbonate (1:1). The cycling tests were automatically carried out with a battery cycler (Maccor 4000). Material handling, cell assembly, test and storage were performed at 20 °C in a dry room (R.H. $< 0.1\%$ at 20 °C).

3. RESULTS

3.1. Chemical-physical characterization

It has been reported that the electrode thickness notably influences the charge/discharge rate capability, energy density,

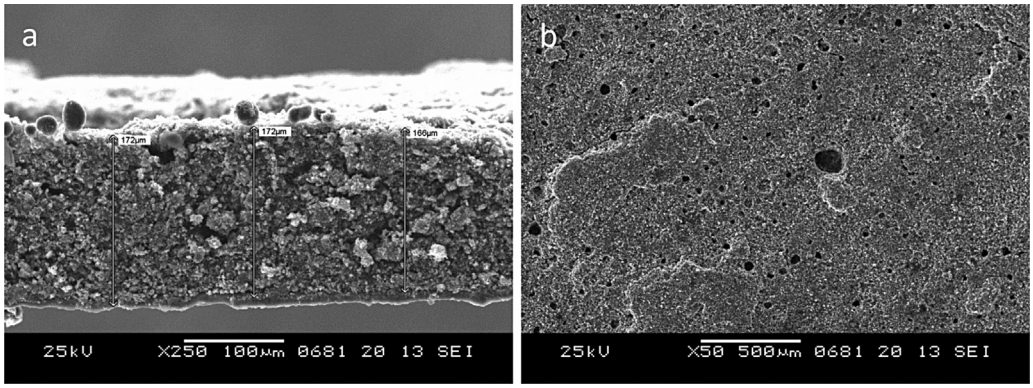

Fig. 1. Scanning electron micrographs of the PVAc-based cathode tape deposited on aluminum current collector. (a) High magnification image (x 250) of the cathode cross section. (b) Low magnification image (x 50) of the cathode surface.

power density, and long-term cycling behavior of $LiFePO_4$ based cathodes [14]. Electrode thickness also has a significant impact on the energy density of the electrode since thicker electrodes can reduce the fraction of inactive materials such as current collectors and separators [15]. The morphology of the as deposited electrode was investigated by scanning electron microscopy. Fig. 1a shows a cross section of the cathode electrode. The electrode appears very uniform in thickness with an average thickness of about 170 micron. Fig. 1b shows a low magnification image of the cathode surface (x 50). The surface depicted in the figure has an area of about 4 mm^2. The surface appears very smooth. Several holes are present on the surface. The presence of the holes makes the electrode very porous. These holes are probably formed during the drying phase due to the release of vapor bubbles which evaporating leave empty spaces into the electrode. To evaluate the electrode porosity, the theoretical and apparent density were calculated. Equation (1) was used to evaluate the theoretical density of the composite electrode [16]:

$$d_t = \frac{1}{\sum_{i=1}^{n} \frac{X_i}{d_{p(i)}}} \quad (1)$$

where: d_t is the theoretical density of the dense electrode (porosity 0%) [g/cm^3], $d_{p(i)}$ is the density of the component i as determined by the helium pycnometer [g/cm^3], and x_i is the weight fraction of the component i. The density of the individual components of the composite electrode, as determined by the helium pycnometer as well as their percentage in the PVAc-based electrode, are reported in Table 1. From these values and using eq. (1) it is possible to calculate the theoretical density of the composite electrode that resulted to be 2.664 g/cm^3.

Equation (2) was used to calculate the geometric density of the electrodes:

$$d_a = \frac{m_s}{v_s} \quad (2)$$

where: d_a is the geometric density of the electrode [g/cm^3], m_s is the mass of the sample [g], and v_s is the volume of the sample [cm^3]. By considering the specific average weight of the electrode (21.0 mg cm^{-2}, excluding the aluminum current collector) and its thickness (0.017 cm), an apparent electrode density of 1.294 g cm^{-3} was calculated.

Equation (3) was used to calculate the electrode porosity:

$$p = \frac{d_t - d_a}{d_t} 100 \quad (3)$$

where: p is the porosity of the electrode [%], d_a is the geometric density of the electrode [g/cm^3] (as evaluated by using eq. 2), and d_t is the theoretical density of the electrode [g/cm^3] (as evaluated by using eq. 1). The porosity of the electrode as calculated by using eq. 3 resulted to be 51%.

Another important parameter that must be kept under close observation during the development of an efficient electrode for lithium-ion battery is the homogeneity and distribution of the various components within the electrode. X-ray EDS was performed in order to study the carbon, oxygen, phosphorus, and iron distribution on the electrode surface. The correspondent distribution maps for a representative area of the electrode surface are depicted in Fig. 2. The iron appears uniformly distributed over the entire surface of the electrode. In contrast, the presence of carbon, oxygen and phosphorus is less evident in some area. This result can be ascribed to the fact that the signal intensity of iron is higher compared to the signal intensity coming from the other three elements. The areas in which carbon, oxygen and phosphorus are less evident are actually areas where the electrode surface is a little bit depressed compared to the other parts of the electrode. As a result, the signal intensity coming from carbon, oxygen and phosphorus is weaker. It should however be noted that, where the signal coming from carbon oxygen and phosphorus is present, the three elements appear uniformly distributed on the electrode surface.

Table 1
Density and percentage of the constituents of the PVAc-based cathode.

Material	$LiFePO_4$	Carbon	PVAc
Density [g/cm^3]	3.56	2.13	1.18
Percentage [wt.%]	75	12.5	12.5

3.2. Thermal characterization

It is known that PVAc degrades in two stages, corresponding to deacetylation and disintegration of the polyolefinic backbone, respectively [17]. The first degradation step lasting up to 400 °C leads to a weight loss of about 72%. The second one occurring up to 450 °C results in nearly 100% weight loss [18]. The TGA and the DTG profiles for the decomposition of PVAc based electrode in nitrogen is shown in Fig. 3. There was no mass loss up to 200 °C. The first stage of degradation, referred to as the acetic acid removal step for PVAc, occurred at temperature between 227 and 375 °C with a maximum centered at 337 °C. The second-stage of degradation followed the first one and ended at 500 °C with a maximum centered at 453 °C. The total weight loss was about 11 wt.% of

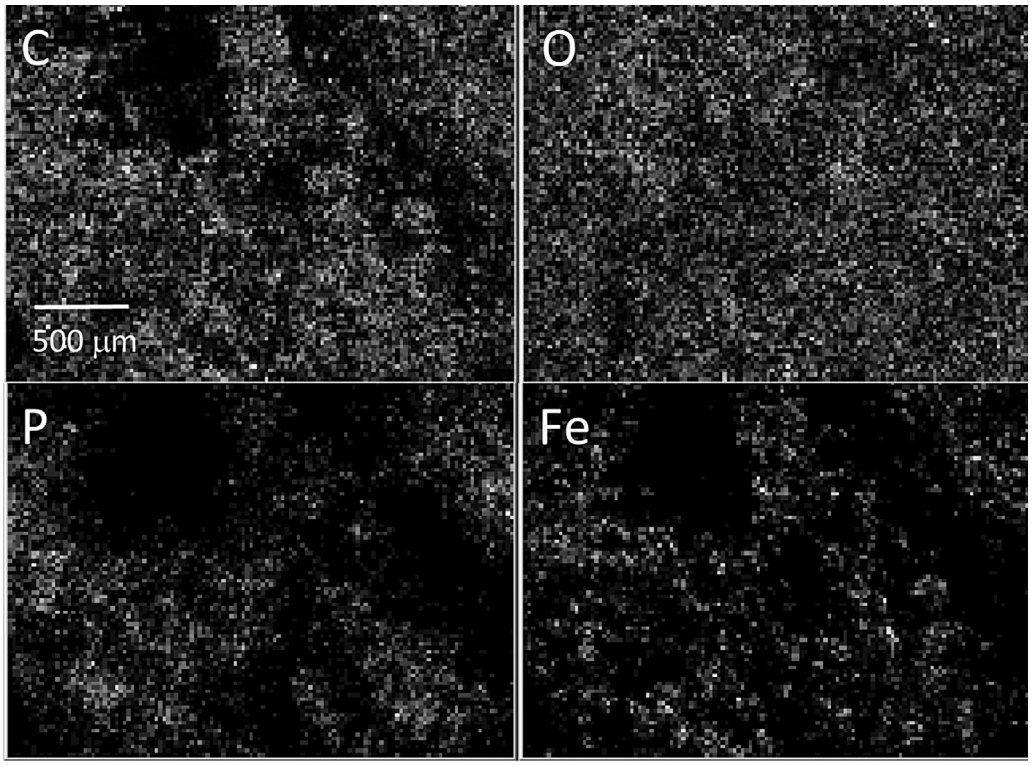

Fig. 2. Distribution maps of the PVAc-based electrode surface for carbon, oxygen phosphorus, and iron as obtained by X-ray energy dispersive spectroscopy.

which about 59% is lost during the first step of degradation while the remaining 41% is lost during the second step. From this results it follows that the PVAc decomposition was slightly affected by the presence of the metal phosphate.

3.3. Electrochemical Characterization

Fig. 4a shows the charge discharge voltage profiles for a PVAc-based electrode. The electrode was cycled for ten cycles at C/10 between 4.2 and 2.0 V. During the first cycle, the electrode was able to de-intercalate all the lithium theoretically contained in its interior. The specific capacity, based on the weight of the active material content in the electrode, was close to the theoretical value (170 mAh g^{-1}). In the following discharge cycle, only a part of lithium extracted during the previous charge was reinserted into the active material and the specific discharge capacity was limited to about 150 mAh g^{-1}. In subsequent cycles this capacity has been reversibly charged and discharged and the charge coefficient (the ratio between the capacity accumulated during the charge and the capacity recovered in the following discharge cycle) reached a value close to the unity (Fig. 4b).

To evaluate the effect of the discharge rate on the specific capacity, the PVAc-based electrode was cycled at different discharge currents corresponding to the rates of C/10, C/5, C, 2C, 3C, and 5C down to 2.0 V. The charge was performed galvanostatically at C rate up to 4.2 Volts, followed by a potentiostatic charging at 4.2 volts until the current decreased to a value equal to C/10. Fig. 5a shows the voltage profiles of the cell. When discharged at C/10 rate, the electrode was able to provide much of its theoretical capacity (150 mAh g^{-1}). By increasing the discharge current, a decrease in the specific capacity and in the average discharge voltage was observed. About 94% of the capacity delivered at C/10 rate is obtained doubling the current (C/5 rate) and the capacity is reduced to 81% at C rate. By further increasing the discharge current the capacity fade is more pronounced: the capacity retention is decreased to about 58% at 2C rate, 44% at 3C rate, and to 35% at 5C rate.

In Fig. 5b is reported the voltage profiles as a function of the specific capacity at various discharge rates for the PVdF-HFP-based electrode. The charge and discharge procedure was the same as reported for the previous described electrode. For discharge rates lower than 2C the electrode showed a behavior similar to that exhibited by the PVAc-based electrode. When discharged at currents higher than C rate, the electrode demonstrated a superior capacity retention but higher cell polarizations. The capacity retention decreased to about 72% at 2C rate and to 77% at 3C rate. At 5C rate the capacity drastically dropped down to 25% of the C/10 capacity.

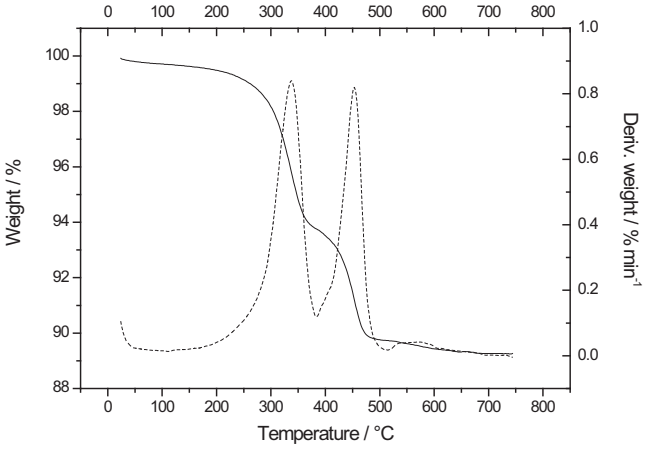

Fig. 3. Termogravimetry (solid line) and differential thermal analysis (dash line) for the PVAc-based electrode conducted from room temperature up to 750 °C at a rate of 10 °C min^{-1} under nitrogen.

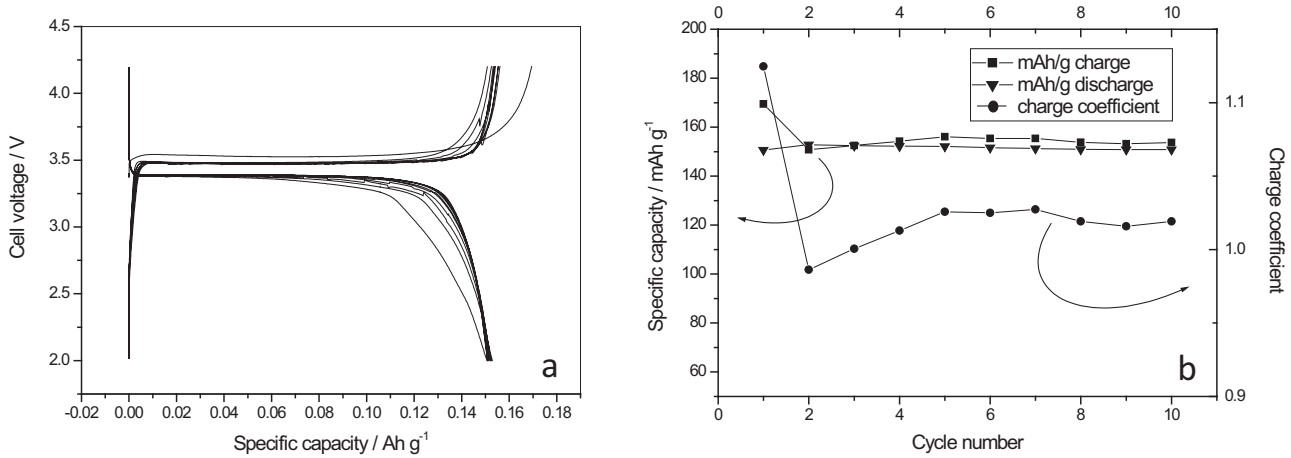

Fig. 4. (a) Voltage profiles as a function of the specific capacity. (b) Specific capacity (in charge and discharge) and charge coefficient as a function of the number of cycles for a PVAc-based electrode cycled in a lithium cell at C/10 rate. The weight of the $LiFePO_4$ active material was 7.6 mg.

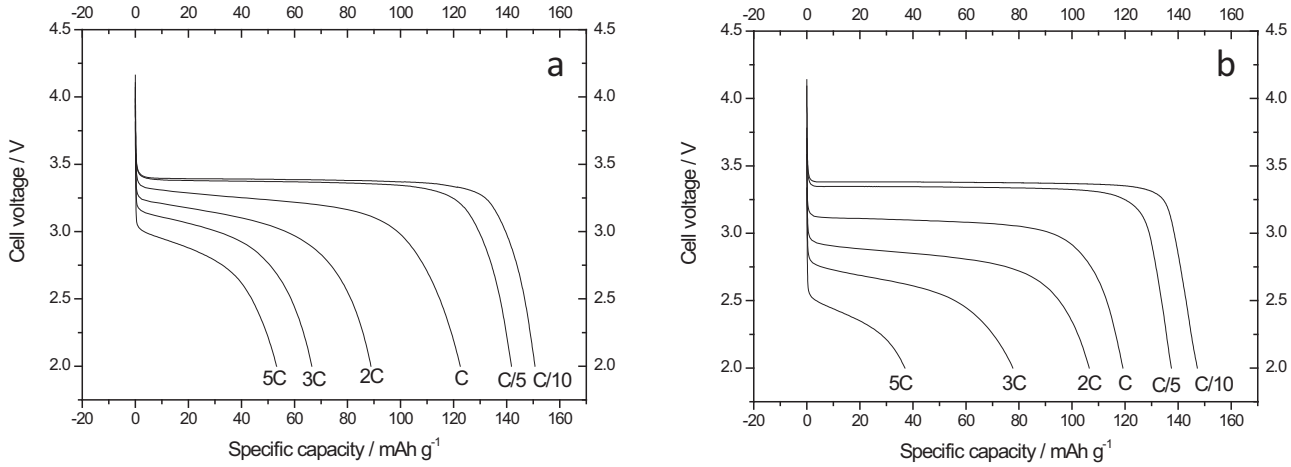

Fig. 5. Voltage profiles as a function of the specific capacity for $LiFePO_4$ electrodes in lithium cells at various discharge rates. The discharge rates are reported in the figure. The cells were charged at C/10 rate. (a) Cell containing the PVAc-based electrode. The weight of the active material is 7.6 mg. (b) Cell containing the PVdF-based electrode. The weight of the active material was 10.4 mg.

An efficient and easy handling methodology to evaluate the performance of thick $LiFePO_4$ composite electrodes was proposed by Fongy et al. [19]. They suggested the use of a parameter k (in hours) to characterize the system response in power. The k parameter is defined by $Q = Q_0 - kI_m$, where Q is the discharge capacity at the specific discharge current I_m (the discharge current divided by the $LiFePO_4$ mass loading, mA g^{-1}), and Q_0 is the equilibrium (very low rate) discharge capacity (mAh g^{-1}). Higher is the k parameter the worst is the electrode performance in term of power. Fig. 6a shows the dependence of the specific capacity as a function of the specific discharge current for the PVAc-based and the PVdF-based electrodes: a linear behaviour was observed and the k parameter was evaluated to be 0.12 h for both the electrodes. This value is in agreement with what found for electrodes with similar capacity density (around 1.5 mA cm^{-2}) and porosity (about 50%) by other authors [19].

The effect of the discharge power on the energy performance of the PVAc-based electrode is summarized in the Ragone plot depicted in Fig. 6b in which the specific energy is reported as a function of the specific power (both calculated on the weight of the active material in the electrode). In the same figure, for comparison, the Ragone plot for the PVdF-based electrode is also reported. The Ragone plot shows that the energy density of the two electrodes follows a similar behavior. The specific energy is reduced from about 500 Wh kg^{-1}, evaluated at a specific power of 56 W kg^{-1}, to about 200 Wh kg^{-1} when the electrodes are discharged at a specific power in excess of 1400 W kg^{-1}. At the higher discharge regime (5C) the specific energy for the PVdF-based electrode declined more rapidly with respect to the PVAc-based electrode due to the reduction of both the specific capacity and the discharge voltage. This result can be ascribed to the fact that active material in the PVdF-based electrode was higher than in the PVAc-based electrode (10.4 mg vs. 7.6 mg).

The rechargeability of the electrode is shown in Fig. 7 where the specific capacity is plotted as a function of the cycle number. The cell was cycled at C rate between 4.2 and 2.0 V. Every 10 cycles a reduced current cycle (C/10) was performed to assess the electrode capacity when discharged under less stressful conditions. The electrode was charged galvanostatically at C rate up to 4.2 V, followed by a potentiostatic charging at 4.2 volts until the current decreased to a value equal to C/10. The cell carried out 80 cycles showing good cyclability. The initial specific capacity at C/10 rate was 125 mAh g^{-1} but the capacity was seen to increase with the number of cycles reaching a value of 135 mAh g^{-1} after 80 cycles. The capacity estimated at C rate ranged between 80 and 90 mAh g^{-1}. The values of the specific capacity exhibited at C/10 and C rate are lower than those previously assessed. Also in this case, the lower capacities are probably related to the fact that the active

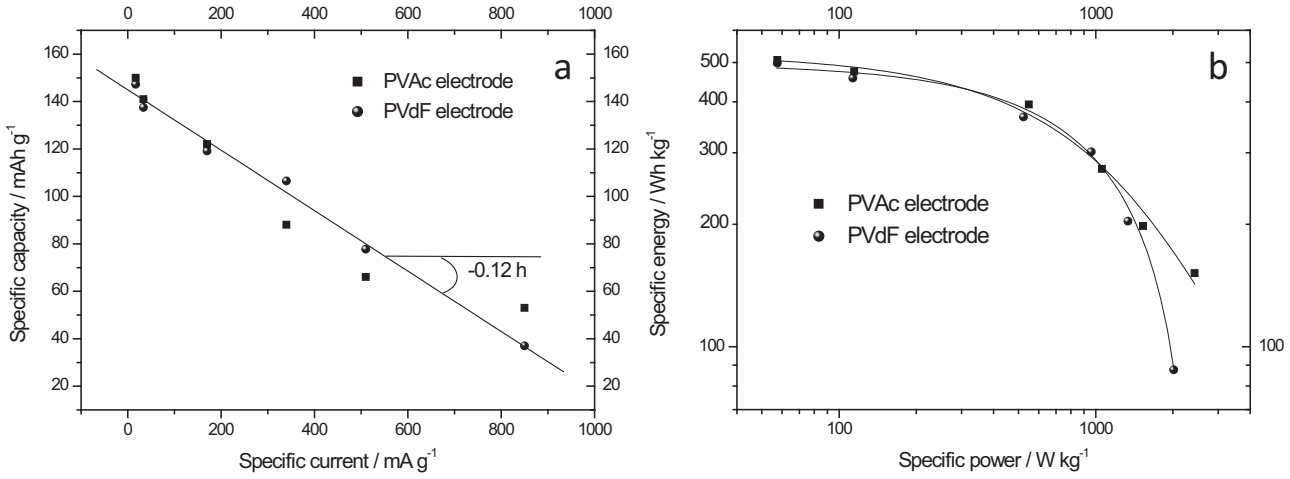

Fig. 6. (a) Specific discharge capacity as a function of the specific discharge current for the PVAc-based (squares) and the PVdF-based (circles) electrodes. (b) Ragone plot for the PVAc-based (squares) and the PVdF-based (circles) electrodes.

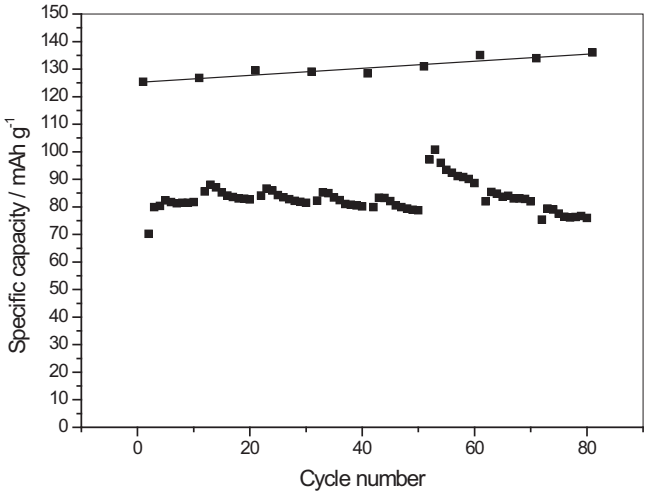

Fig. 7. Specific capacity as a function of the number of cycles for a $LiFePO_4$ electrode based on PVAc cycled at C rate in a lithium cell. Every 10 cycles a reduced current cycle (C/10 rate) was carried out. The electrode was charged galvanostatically at C rate up to 4.2 Volts, followed by a potentiostatic charging at 4.2 volts until the current decreases to a value equal to C/10. The weight of the active material was 13.2 mg.

material in the electrode was higher with respect to the previously tested electrode (13.2 mg vs. 7.6 mg).

4. CONCLUSION

In this work, for the first time, the use of PVAc as a binder in the formulation of a $LiFePO_4$ based-electrode for lithium-ion batteries is described. A suspension of the active material, carbon and PVAc was used to paint a thin aluminum sheet. The so obtained electrode possesses an appropriate porosity to allow the electrolyte to penetrate in its inside. The electrode has shown interesting electrochemical properties making it suitable for the realization of high-energy/high power lithium-ion batteries. The electrode can be discharged at C/10 rate providing about 150 mAh g^{-1}. By increasing the discharge rate the capacity decreases but at least 30% of the capacity is still available when the electrode is discharged at 5C rate. The electrochemical behavior is comparable to that observed for a conventional PVdF-based electrode. The electrode properties can be outlined by considering the electrochemical performance of the active material in terms of specific capacity (150 mAh g^{-1} @ C/10 rate), specific energy (500 Wh kg^{-1} @ C/10 rate), specific power (2400 W kg^{-1} @ 5 C rate) and negligible loss of capacity with the progress of the number of cycles.

ACKNOWLEDGMENTS

Part of this work was carried out within the activities “Ricerca Sistema Elettrico” funded through contributions to research and development by the Italian Ministry of Economic Development.

Appendix A. Supplementary data

Supplementary data associated with this article can be found, in the online version, at http://dx.doi.org/10.1016/j.electacta.2014.10.123.

References

[1] W. Porcher, B. Lestriez, S. Jouanneau, D. Guyomard, Optimizing the surfactant for the aqueous processing of $LiFePO_4$ composite electrodes, J. Power Sources 195 (2010) 2835–2843.
[2] Commission Directive 2009/2/EC, 31st Adaptation to Technical Progress to the Dangerous Substances Directive, Annex 1 of the Dangerous Substances Directive (67/548/EEC), Official Journal of the European Union (2009) L11/15.
[3] S.F. Lux, F. Schappacher, A. Balducci, S. Passerini, M. Winter, Low Cost, Environmentally Benign Binders for Lithium-Ion Batteries, J. Electrochem. Soc. 157 (2010) A320–A325.
[4] J.H. Lee, H.H. Kim, D.S. Zang, Y.M. Choi, H. Kim, D.K. Yi, W.M. Sigmund, U. Paik, Evaluation of Surface Acid and Base Properties of $LiFePO_4$ in Aqueous Medium with pH and Its Electrochemical Properties, J. Phys. Chem. C 114 (2010) 4466–4472.
[5] W. Porcher, P. Moreau, B. Lestriez, S. Jouanneau, D. Guyomard, Is $LiFePO_4$ stable in water? Toward greener li-ion batteries, Electrochem. Solid State Lett. 11 (2008) A4–A8.
[6] W. Porcher, P. Moreau, B. Lestriez, S. Jouanneau, F. Le Cras, D. Guyomard, Stability of $LiFePO_4$ in water and consequence on the Li battery behavior Ionics 14 (2008) 583–587.
[7] W. Porcher, B. Lestriez, S. Jouanneau, D. Guyomard, Design of Aqueous Processed Thick $LiFePO_4$ Composite Electrodes for High-Energy Lithium Battery, J. Electrochem. Soc. 156 (3) (2009) A133–A144.
[8] M. Guerfi, Kaneko, M. Petitclerc, M. Mori, K. Zaghib, $LiFePO_4$ water-soluble binder electrode for Li-ion batteries, J. Power Sources 163 (2007) 1047–1052.
[9] J.-H. Lee, J.-S. Kim, Y.C. Kim, D.S. Zang, U. Paik, Dispersion properties of aqueous-based $LiFePO_4$ pastes and their electrochemical performance for lithium batteries, Ultramicroscopy 108 (2008) 1256–1259.
[10] C.-C. Li, Y.-H. Wang, T.-Y. Yang, Effects of Surface-coated Carbon on the Chemical Selectivity for Water-Soluble Dispersants of $LiFePO_4$, J. Electrochem. Soc. 158 (2011) A828–A834.
[11] C.-C. Li, X.-W. Peng, J.-T. Lee, F.-M. Wang, Using Poly(4-Styrene Sulfonic Acid) to Improve the Dispersion Homogeneity of Aqueous-Processed $LiFePO_4$ Cathodes, J. Electrochem. Soc. 157 (2010) A517–A520.

[12] M. Sun, H. Zhong, S. Jiao, H. Shao, L. Zhang, Investigation on Carboxymethyl Chitosan as New Water Soluble Binder for $LiFePO_4$ Cathode in Li-Ion Batteries, Electrochimica Acta 127 (2014) 239–244.
[13] Deutsche Reichs Patent no. 281687 (4 July 1913), an abstract of which appears in the Journal of the Society of Chemical Industry (London), vol. 34, page 623 (1915).
[14] H. Zheng, J. Li, X. Song, G. Liu, V.S. Battaglia, A comprehensive understanding of electrode thickness effects on the electrochemical performances of Li-ion battery cathodes, Electrochim. Acta 71 (2012) 258–265.
[15] D.Y.W. Yu, K. Donoue, T. Inoue, M. Fujimoto, S. Fujitani, Effect of Electrode Parameters on $LiFePO_4$ Cathodes, J. Electrochem. Soc. 153 (2006) A835–A839.
[16] G.B. Appetecchi, M. Carewska, F. Alessandrini, P.P. Prosini, S. Passerini, Characterization of PEO-based composite cathodes - I. Morphological, thermal, mechanical, and electrical properties, J. Electrochem. Soc. 147 (2000) 451–459.
[17] T. Uyar, A.E. Tonelli, J. Hacaloğlu, Thermal degradation of polycarbonate, poly (vinyl acetate) and their blends, Polym. Degrad. Stab. 91 (2006) 2960–2967.
[18] J. Blazevska-Gilev, D. Spaseska, Thermal Degradation of PVAc, J. Univers. Chem. Tech. Metall. 40 (2005) 287–290.
[19] C. Fongy, A.C. Gaillot, S. Jouanneau, D. Guyomard, B. Lestriez, Ionic vs Electronic Power Limitations and Analysis of the Fraction of Wired Grains in $LiFePO_4$ Composite Electrodes, J. Electrochem. Soc. 157 (2010) A885–A891.